Lifting of nodes by disorder in extended-*s*-state superconductors: Application to ferropnictides

V. Mishra,[1] G. Boyd,[1] S. Graser,[1,2] T. Maier,[3] P. J. Hirschfeld,[1] and D. J. Scalapino[4]
[1]*Department of Physics, University of Florida, Gainesville, Florida 32611, USA*
[2]*Center for Electronic Correlations and Magnetism, Institute of Physics, University of Augsburg, D-86135 Augsburg, Germany*
[3]*Center for Nanophase Materials Sciences and Computer Science and Mathematics Division, Oak Ridge National Laboratory, Oak Ridge, Tennessee 37831-6494, USA*
[4]*Department of Physics, University of California–Santa Barbara, Santa Barbara, California 93106-9530 USA*
(Received 19 January 2009; revised manuscript received 9 February 2009; published 11 March 2009)

We show, using a simple model, how ordinary disorder can gap an extended-*s*- (A_{1g}) symmetry superconducting state with nodes. The concomitant crossover of thermodynamic properties, particularly the T dependence of the superfluid density, from pure power-law behavior to an activated one is exhibited. We discuss applications of this scenario to experiments on the ferropnictide superconductors.

DOI: 10.1103/PhysRevB.79.094512 PACS number(s): 74.20.−z, 74.62.−c, 74.25.−q

I. INTRODUCTION

When a new class of unconventional superconductors is discovered, it is traditional to try to determine the symmetry class of the order parameter, as this may provide clues as to the nature of the pairing mechanism. Direct measurements of the superconducting order parameter are not possible, and indirect phase-sensitive measurements are sometimes difficult because they typically involve high-quality surfaces.[1] On the other hand, a set of relatively straightforward experimental tests are available to determine the existence of low-energy quasiparticle excitations and, in some cases, their distribution in momentum space. As in earlier experiences with other candidate unconventional systems such as the high-T_c cuprates and heavy-fermion materials, the symmetry class of the newly discovered ferropnictide superconductors[2] is in dispute at this writing, due in part to differing results on superfluid density,[3–9] angle-resolved photoemission spectroscopy (ARPES),[10–15] nuclear magnetic resonance (NMR),[16–20] Andreev spectroscopy,[21–24] and other probes. In some cases, results have been taken to indicate the absence of low-energy excitations, i.e., a fully developed spectral gap. In others, low-energy power laws have been taken as indication of the existence of order-parameter nodes. It is not yet clear whether these differences depend on the stoichiometry or doping of the materials, or possibly on sample quality.

In parallel, microscopic theoretical calculations of the pairing interaction in the ferropnictide materials have attempted to predict the momentum dependence of the order parameter associated with the leading superconducting instability. Using a five-orbital parameterization of the density-functional theory (DFT) band structure, Kuroki *et al.*[25] performed a random phase approximation (RPA) calculation of the spin and orbital contributions to the interaction to construct a linearized gap equation. They found that the leading pairing instability had *s*-wave (A_{1g}) symmetry, with nodes on the electronlike Fermi surface ("β sheets"), and noted that the next leading channel had $d_{x^2-y^2}(B_{1g})$ symmetry. Wang *et al.*[26] studied the pairing problem using the functional renormalization-group approach within a five-orbital framework, also finding that the leading pairing instability is in the *s*-wave channel, and that the next leading channel has $d_{x^2-y^2}$ symmetry. For their interaction parameters, they found however that there were no nodes on the Fermi surface, but there was a significant variation in the magnitude of the gap. Other approaches have obtained A_{1g} gaps which change sign between the hole and electron Fermi-surface sheets but remain approximately isotropic on each sheet.[27,28]

We also recently presented calculations of the spin and charge fluctuation pairing interaction within a five-orbital RPA framework,[29] using the DFT band structure of Cao *et al.*[30] as a starting point. Our results indicated that the leading pairing channels were indeed of $s(A_{1g})$ and $d_{x^2-y^2}$ symmetry and that one or the other could be the leading eigenvalue, depending on details of interaction parameters. We also gave arguments as to why these channels were so nearly degenerate, and pointed out some significant differences in the states compared to those found by Kuroki *et al.*[25] Finally, we noted that within our treatment and for the interaction parameter space explored, nodes were found in all states, generally on the α sheets for the *d*-wave case and the β sheets for the *s*-wave case, but that in the latter case the excursion of the order parameter of sign opposite to the average sign on the sheet was small and might be lifted by disorder.[29]

It is the purpose of this paper to explore the possibility that the nodes of an extended-*s* state of the type discussed in Ref. 29 are lifted by disorder, and consider the consequences for experimental observables. By "lifting" of nodes, we mean specifically the gapping of the low energy spectrum near the Fermi level. In the interest of simplicity, we initially neglect many complicating aspects of the problem, in particular the multisheet nature of the Fermi surface, and focus primarily on the sheet found in each case (*s* or *d*) which has nodes. In this case the problem is similar to one which was studied earlier in the context of potential extended-*s* states in a single-band situation for cuprate superconductors.[31–33] For the pnictides, current interest centers around the isotropic sign-changing extended-*s* state proposed by Mazin *et al.*,[27] one where the gap is momentum independent over two independent Fermi-surface sheets, but has a different sign on each. In this case, it is known that only interband scattering is pairbreaking because it mixes the two signs and suppresses the overall order parameter.[33–36] This effect has been claimed

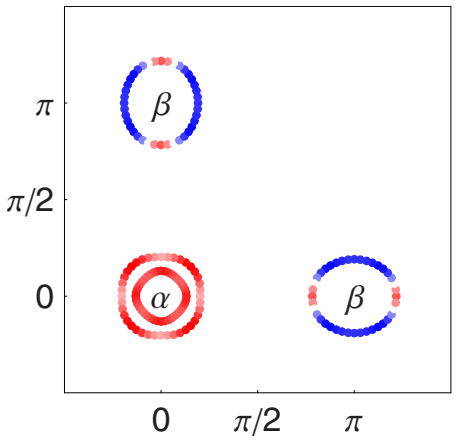

FIG. 1. (Color online) Fermi surface and extended-*s*-gap eigenfunction from Fig. 15(d) of Ref. 29. Red/blue color indicates sign of order parameter.

to account for low-energy excitations observed in NMR (Refs. 37 and 38) and superfluid density[39] experiments. In general, impurities with screened Coulomb potential will have a larger intraband component, which is however essentially irrelevant for the isotropic case in the sense of Anderson's theorem. However, intraband scattering by disorder will average any anisotropy of the order parameter present in the conventional *s*-wave case.[40] In the case of the pnictides, this intraband component will do the same, with the effect of lifting the weak nodes found in our microscopic calculations. We demonstrate this effect, and its consequences, within a simple model where we take weak pointlike scatterers, treated in the Born approximation, as a model for the intraband part of the true disorder scattering in the pnictides. We believe that such scattering arises primarily from out-of-plane dopants such as K in the hole-doped materials and F in the electron-doped materials; since these dopants sit away from the FeAs plane, they will certainly produce a significant small-**q** component of the scattering potential, which will mix states on the same sheet. Our results suggest that an extended-*s* wave state with nodes, lifted by disorder in the case of the doped superconducting ferropnictides, may explain the apparent discrepancies among various measurements in the superconducting states of these materials.

II. MODEL

We begin by assuming a superconductor with a separable pair interaction $V(\mathbf{k},\mathbf{k}')=V_1\Phi_1(\phi)\Phi_1(\phi')$, where ϕ is an angle parametrizing the electronic momentum $\mathbf{k}$ on a single circular Fermi surface. To model a situation corresponding to an extended-*s* state on the β sheet of the Fe-pnictide materials (see Fig. 1), as found in Ref. 29, we choose

$$\Phi_1(\phi) = 1 + r\cos 2\phi, \tag{1}$$

with $r \equiv V'/V_1 \gtrsim 1$, ensuring that the pure order parameter $\Delta_{\mathbf{k}}=\Delta_0\Phi_1(\phi)$ will have nodes near $\phi=\pi/4,3\pi/4,\ldots$. Note that this function is also suitable for modeling the *d*-wave state on the α Fermi-surface sheets, in the limit $r \gg 1$. Because the effect of disorder will renormalize the constant and $\cos 2\phi$ parts of the order parameter differently, we write it in the general case as $\Delta_{\mathbf{k}}=\Delta_0+\Delta'\cos 2\phi$.

The full matrix Green's function in the presence of scattering in the superconducting state is

$$G(\mathbf{k},\omega) = \frac{\tilde{\omega}\tau_0 + \tilde{\epsilon}_{\mathbf{k}}\tau_3 + \tilde{\Delta}_{\mathbf{k}}\tau_1}{\tilde{\omega}^2 - \tilde{\epsilon}_{\mathbf{k}}^2 - \tilde{\Delta}_{\mathbf{k}}^2}, \tag{2}$$

where $\tilde{\omega} \equiv \omega - \Sigma_0$, $\tilde{\epsilon}_{\mathbf{k}} \equiv \epsilon_{\mathbf{k}} + \Sigma_3$, $\tilde{\Delta}_{\mathbf{k}} \equiv \Delta_{\mathbf{k}} + \Sigma_1$, and Σ_α are the components of the self-energy proportional to the Pauli matrices τ_α in particle-hole (Nambu) space. If we assume weak scattering, we may approximate the self-energy in the Born approximation as

$$\underline{\Sigma} = n_I \sum_{k'} |U(\mathbf{k}\mathbf{k}')|^2 \tau_3 \underline{G}^0(\mathbf{k}',\omega)\tau_3, \tag{3}$$

where n_I is the concentration of impurities. The self-energy has Nambu components

$$\Sigma_0(\mathbf{k},\omega) = n_I \sum_{\mathbf{k}'} |U(\mathbf{k},\mathbf{k}')|^2 \frac{\tilde{\omega}}{\tilde{\omega}^2 - \tilde{\epsilon}_{\mathbf{k}'}^2 - \tilde{\Delta}_{\mathbf{k}'}^2}, \tag{4}$$

$$\Sigma_3(\mathbf{k},\omega) = n_I \sum_{\mathbf{k}'} |U(\mathbf{k},\mathbf{k}')|^2 \frac{\tilde{\epsilon}_{\mathbf{k}'}}{\tilde{\omega}^2 - \tilde{\epsilon}_{\mathbf{k}'}^2 - \tilde{\Delta}_{\mathbf{k}'}^2}, \tag{5}$$

and

$$\Sigma_1(\mathbf{k},\omega) = -n_I \sum_{\mathbf{k}'} |U(\mathbf{k},\mathbf{k}')|^2 \frac{\tilde{\Delta}_{\mathbf{k}'}}{\tilde{\omega}^2 - \tilde{\epsilon}_{\mathbf{k}'}^2 - \tilde{\Delta}_{\mathbf{k}'}^2}. \tag{6}$$

As discussed above, we assume pointlike impurity scattering $U(\mathbf{k},\mathbf{k}')=U_0$, and treat the disorder in Born approximation. We further assume particle-hole symmetry such that $\Sigma_3=0$, leading to Nambu self-energy components[41] after integration perpendicular to the Fermi surface,

$$\Sigma_0(\phi,\omega) = \Gamma \left\langle \frac{\tilde{\omega}}{\sqrt{\tilde{\omega}^2 - \tilde{\Delta}_{\mathbf{k}'}^2}} \right\rangle_{\phi'}, \tag{7}$$

$$\Sigma_1(\phi,\omega) = -\Gamma \left\langle \frac{\tilde{\Delta}_{\mathbf{k}'}}{\sqrt{\tilde{\omega}^2 - \tilde{\Delta}_{\mathbf{k}'}^2}} \right\rangle_{\phi'}, \tag{8}$$

where $\langle\,\rangle_\phi$ indicates averaging over the circular Fermi surface and $\Gamma=\pi n_I N_0 U_0^2$ is the normal-state scattering rate, with N_0 the density of states at the Fermi level.

III. RESULTS

The Bardeen-Cooper-Schrieffer (BCS) gap equation

$$\Delta_{\mathbf{k}} = \frac{1}{2}\mathrm{Tr}\, T\sum_{\omega_n}\sum_{\mathbf{k}'} V_{\mathbf{k},\mathbf{k}'}\tau_1 G(\mathbf{k}',\omega_n) \tag{9}$$

then reduces to

$$\Delta_0 = N_0[V_1\Delta_0 I_1 + (V'\Delta_0 + V_1\Delta')I_2 + V'\Delta' I_3],$$

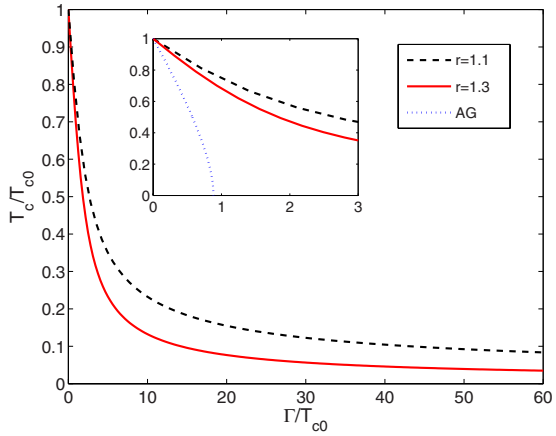

FIG. 2. (Color online) Suppression of the critical temperature T_c/T_{c0} vs normal-state scattering rate Γ/T_{c0} for anisotropy parameter $r=1.1$ (dashed), 1.3 (solid). The inset shows the two curves at smaller values of the scattering rate. The T_c suppression curve expected from Abrikosov-Gor'kov theory (Ref. 41) (dotted) is included for comparison.

$$\Delta' = N_0[V'\Delta_0 I_1 + (V'\Delta' + rV'\Delta_0)I_2 + rV'\Delta' I_3] \quad (10)$$

with

$$I_m = \pi T \sum_{\omega_n} \left\langle \frac{(\cos 2\phi)^{m-1}}{\sqrt{\tilde{\omega}_n^2 + \tilde{\Delta}_{\mathbf{k}'}^2}} \right\rangle_{\phi'}, \quad (11)$$

and where $\omega_n=(2n+1)\pi T$ is a fermionic Matsubara frequency.

A. T_c suppression

Near T_c, $I_1=\mathcal{L}$, $I_2=0$ and $I_3=\mathcal{L}/2$, where $\mathcal{L}=\log[\frac{2e^{\gamma}\omega_c}{\pi T_c}]$, leading to a critical temperature of

$$T_c = 1.13\omega_c \exp\left[-\frac{V_1}{N_0(V_1^2 + V'^2/2)}\right] \quad (12)$$

in the clean limit. In the dirty case, T_c is suppressed by ordinary disorder until the gap anisotropy is completely washed out, at values of the normal-state scattering rates Γ many times larger than T_c, as also found by Markowitz and Kadanoff,[40] using the theory of Abrikosov and Gor'kov.[41] In Fig. 2, we plot this behavior by solving Eq. (11) with Φ_1 given by Eq. (1). The marginal case $r=1$ describes the situation where the nodes just touch the Fermi surface without disorder, which has been discussed earlier.[31] Note that while the scale of the plot implies that the critical temperature is rapidly suppressed, the scattering rate scale over which this occurs is actually much greater than one would expect in, e.g., a d-wave superconductor, where a critical concentration $\Gamma_c \sim T_{c0}$ suffices to suppress superconductivity completely.

B. Density of states and spectral gap

In the symmetry broken state, the order parameter $\Delta_{\mathbf{k}}$ is renormalized by the off-diagonal self-energy $\Sigma_1(\mathbf{k},\omega)$, but the true spectral gap is determined by both Nambu components Σ_1 and Σ_0. One may define an angle-dependent spectral gap $\Omega_G(\phi)$ by examining the one-particle spectral function $A(\mathbf{k},\omega) \equiv -(1/\pi)\mathrm{Im}\, G_{11}(\mathbf{k},\omega)$, and plotting either the peak or the energy between the peak and the Fermi level where A falls to one half its peak value. We adopt the latter definition here since it is similar to one traditionally used in the ARPES community, but other measures [e.g., plotting the peak in $A(\mathbf{k},\omega)$ or simply $\tilde{\Delta}(\omega=0,\phi)$] produce very similar results. Note that in the clean limit, the spectral gap reduces to the order parameter, $\Omega_G(\phi) \to \Delta_{\mathbf{k}}$.

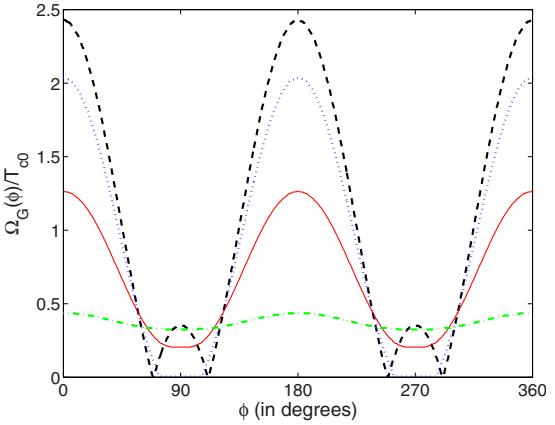

FIG. 3. (Color online) Normalized spectral gap $\Omega_G(\phi)/T_{c0}$ vs angle ϕ on the Fermi surface for an extended s-wave state with $r=1.3$ and $\Gamma/T_{c0}=0$ (dashed), 0.3 (dotted), 1.0 (solid), and 3.1 (dashed-dotted).

In Fig. 3, we show the s-wave spectral gap plotted over the Fermi surface for various values of the scattering rate Γ. It is clear that the effect of scattering is as described above: the order parameter is averaged over the Fermi surface, which eventually has the effect of lifting the nodes, and leading to a true gap in the system, which becomes isotropic at sufficiently large scattering rates. Note this is quite different from what happens in a superconductor with nodes which exist due to the unconventional symmetry class of the system, e.g. the well-known $d_{x^2-y^2}$ state. In such a case, the spectral gap extrema are simply suppressed by disorder, without any true gapping of the excitation spectrum. A superconducting state of a given symmetry class can, however, have additional nodes due to nongeneric structures in the pairing interaction which are consistent with that class.[44] The simplest example thereof is the A_{1g} representation we consider here, which has basis functions which must have the full symmetry of the crystal lattice, but which have no further general restrictions; details depend on the pair interaction. In particular, they may manifest nodes, which may be lifted by nonmagnetic disorder.[31,32]

The lifting of nodes can be observed as well in the total density of states (DOS), which we exhibit in Fig. 4. In the clean situation, there are two coherence-type peaks, corresponding to the large and small antinodal order-parameter scales observed in Fig. 3. The addition of disorder initially smears these peaks, suppresses the maximum gap feature, and leads to a constant DOS at the Fermi level. This is consistent with the expected behavior of a dirty nodal superconductor.[42,43] This behavior continues until the point

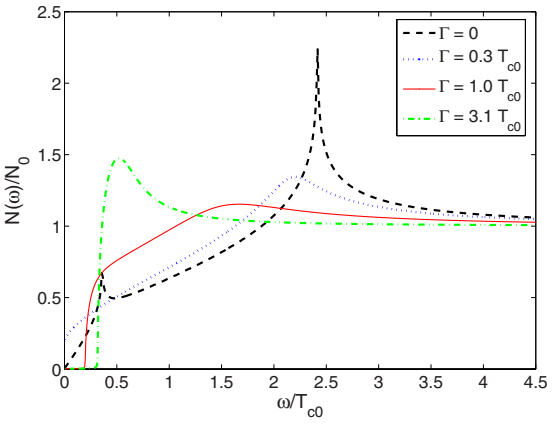

FIG. 4. (Color online) Normalized density of states $N(\omega)/N_0$ vs energy ω for the same parameters and line types as Fig. 3.

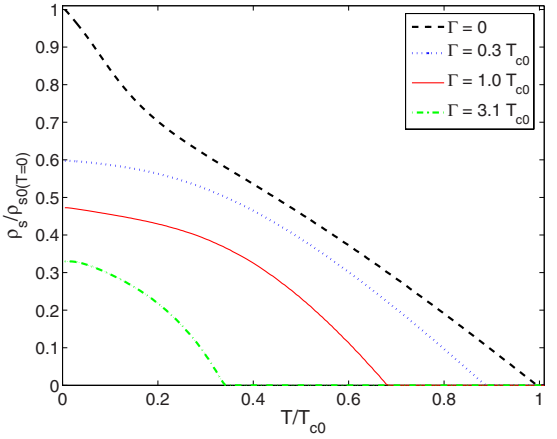

FIG. 5. (Color online) Superfluid density ρ_s/m^* vs T/T_{c0} for $r=1.3$ and same disorder parameters and line types as in Figs. 3 and 4.

when the nodes are actually lifted, and the system acquires a true gap, at which point the peak begins to sharpen again (see Fig. 4). When the gap has become completely isotropic due to disorder averaging, the DOS is identical to the usual clean limit BCS DOS, as required by Anderson's theorem.

C. Superfluid density

The temperature dependence of the superfluid density $\rho_s(T)$ reflects the distribution of quasiparticle states which contribute to the normal-fluid fraction. Early data on powdered samples of R-FeAsO$_x$F$_{1-x}$ [R=Pr,[3] Sm,[4] Nd (Ref. 5)] near optimal doping showed exponential T dependence, as did measurements on $Ba_xK_{1-x}Fe_2As_2$ (Ba-122).[6] More recent experiments on the latter system doped with Co found a power-law temperature dependence close to T^2, which evolved towards exponential behavior with increasing Co concentration.[8] A T^2 dependence is characteristic of a dirty system with linear nodes,[49] but the authors of Ref. 8 concluded the T^2 was more likely due to nonlocal electrodynamics[50] or pairbreaking due to inhomogeneity or inelastic scattering. Very recently, however, a *linear T* dependence was measured in the original ferropnictide superconductor LaFePO,[51] with T_c=6 K. Because this material is stoichiometric, crystals have very long mean-free paths of more than a thousand Angström and are capable of supporting de Haas-van Alphen (dHvA) oscillations.[52] It seems very unlikely that anything but order-parameter nodes can lead to such a power law. The pure s-wave state we consider here with weak nodes will immediately yield $\rho_s(0)-\rho_s(T)\sim T$, so we take the parameters of the previous section and calculate ρ_s directly.

Within the current BCS-type model, the xx component of the superfluid density tensor ρ_s may be written

$$\rho_{s,xx}/\rho = \left\langle \cos^2\phi \int d\omega \tanh\frac{\omega}{2T}\mathrm{Re}\frac{\tilde{\Delta}_{\mathbf{k}}^2}{(\tilde{\omega}^2-\tilde{\Delta}_{\mathbf{k}}^2)^{3/2}}\right\rangle_{\phi}, \tag{13}$$

where ρ is the full electron density. Note this standard expression for the superfluid density of a dirty superconductor[45] is complete within mean-field theory since vertex corrections to the current response vanish for singlet superconductors and pointlike scatterers.[46] In Fig. 5, we show the superfluid density $\bar{\rho}_s \equiv (\rho_{s,xx}+\rho_{s,yy})/2$ calculated from Eq. (13) vs temperature for various scattering rates.[47] In the pure system, the superfluid density is linear at the lowest temperatures, reflecting the existence of line nodes. At a temperature corresponding to the smaller antinodal gap,[48] there is a decrease in the rate at which thermally excited quasiparticles depopulate the condensate, and therefore a change in slope as visible in the figure. We note that this kinklike behavior may disappear when excitations from other Fermi-surface sheets which contribute at higher temperatures are included, but also that this type of upward curvature in ρ_s vs T was observed by Fletcher *et al.*[9] in the cleanest LaFePO samples.

If disorder is now added without lifting the nodes, the generic behavior will be quadratic in temperature,[49] i.e., $\rho_s \simeq \rho_s(0)(1-aT^2/\Gamma^2)$, where a is a constant of order unity. When the nodes are completely lifted, an exponential T dependence, $\rho_s \simeq \rho_s(0)[1-a\exp(-\Delta_{\min}/T)]$ must dominate at the lowest temperatures. These power laws are displayed more precisely in the log-log plot of Fig. 6. The pure system follows a linear-T law $[\rho_s(0)-\rho_s(T)\sim T]$ down to the lowest temperatures, as expected because of the linear nodes, whereas the dirty systems follow a T^2 law over an intermediate T range, also expected because the states are uniformly broadened in this range by Born scattering with $1/\tau$ roughly linear in energy. At lower temperatures, however, the dirty cases no longer exhibit power laws in temperature, with the curves showing fully developed gaps in Fig. 4 following activated behavior. The Γ/T_{c0}=0.3 case is marginal in the sense that the effective spectral gap has nodes which just touch the Fermi surface, and the figure shows that when the system is close to this condition the low-T behavior is not a simple power law or exponential.

IV. EFFECT OF ADDITIONAL FERMI-SURFACE SHEETS

While the desired effect of node lifting by disorder for an extended-s wave state with weak nodes has now been exhib-

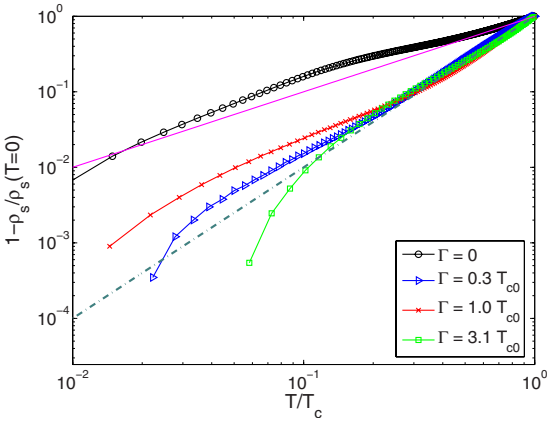

FIG. 6. (Color online) $\log_{10}(1-\rho_s(T)/\rho_s(0))$ vs $\log_{10} T/T_c$ for $r=1.3$ and various scattering rates. Circles: $\Gamma=0$, triangles: $\Gamma/T_{c0}=0.3$, crosses: $\Gamma/T_{c0}=1.$, and squares: $\Gamma/T_{c0}=3.1$. Solid line: T; dashed-dotted line: T^2.

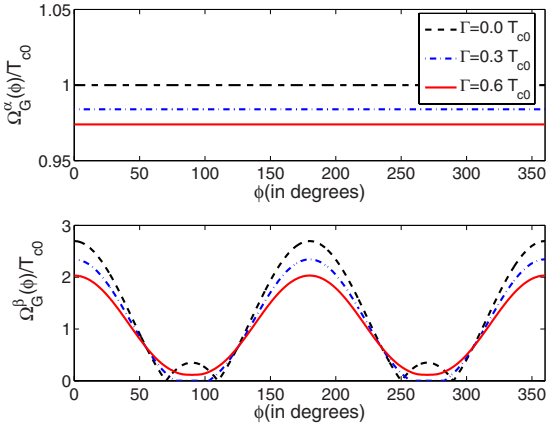

FIG. 7. (Color online) Spectral gaps $\Omega_G(\phi)/T_{c0}$ vs ϕ for the α (top) and β (bottom) sheets for the two-band model. Here the pairing parameters $V_{11}=1.0, V_{12}=-0.6, V_{22}=1.5$ were chosen so that $r_{\text{eff}}=1.3$ is the same as in the one-band case. The densities of states ratio was taken as $N_2(0)/N_1(0)=1.25$. Scattering rates for intraband scattering correspond to $\Gamma \equiv n_i \pi N_1(0)|U_{11}|^2=0$ (dashed), 0.3 (dashed-dotted), 0.6 (solid).

ited, the amount of disorder required to lift the nodes has also been shown to suppress T_c substantially. As strong sample-to-sample variations in T_c have not been observed in the ferropnictides, this seems inconsistent with the current overall body of experimental data. There are several possibilities to explain this discrepancy. The first is that the nodes, e.g., in the LaFePO system, may be accidentally extremely weak. This seems unlikely since the linear-T behavior extends over a significant fraction of T_c in this material. Were the nodes to be marginal or extremely weak, the phase space from near-quadratic nodes would actually lead to a $T^{1/2}$ temperature variation in the penetration depth in the pure system, which is not observed. We have also examined the above model with smaller values of $r \gtrsim 1$, and find that substantial scattering rates are still required to create a significant spectral gap.

It is possible that our restriction to Born (weak) scattering is inadequate. Unitary scatterers modify primarily the states near the nodes, creating a gap without affecting the states at higher energies; smaller normal-state scattering rates can therefore produce a large node lifting effect without suppressing T_c significantly.[53] It may be interesting to explore this effect further, but *a priori* there is no obvious reason for the out-of-plane impurities which appear to dominate the K-doped pnictide materials to produce such strong scattering potentials.

A final possibility, which we do pursue here, is that in the ferropnictides, the single Fermi-surface sheet we have studied thus far is coupled to other sheets which control the T_c suppression. This appears plausible within the context of our microscopic spin-fluctuation pairing calculations,[29] which show that for extended-s-type states, while the β sheets appear to have weak nodes, the α sheets are more isotropic for the extended-s-wave solutions. The pairing on the α and β sheets is strongly coupled by the $\pi,0$ (unfolded zone) scattering processes which dominate the spin-fluctuation spectrum. To suppress the critical temperature, it is clear that not only the β condensate, but also the α condensate must be suppressed. The α condensate may therefore be expected to act as a reservoir which maintains the critical temperature (provided interband scattering by disorder is relatively weak), while the β condensate is nodal and therefore dominates low-temperature and low-energy properties.

To test this hypothesis within the philosophy of the current paper, we take the above model and add to it a single additional sheet with constant pairing amplitude, and couple the two sheets by constant pairing potentials, leading to a total pairing interaction.

$$V(\mathbf{k},\mathbf{k}') = V_1\Phi_1(\mathbf{k})\Phi_1(\mathbf{k}') + V_2\Phi_2(\mathbf{k})\Phi_2(\mathbf{k}') + V_{12}[\phi_1(\mathbf{k})\phi_2(\mathbf{k}') + \phi_2(\mathbf{k})\phi_1(\mathbf{k}')], \quad (14)$$

where $\phi_1(\mathbf{k})=1+r\cos 2\phi$ is understood as before to describe states with $\mathbf{k}$ on the β sheet, whereas $\phi_2(\mathbf{k})=1$ for $\mathbf{k}$ on the α sheet. Note that V_{12} is chosen of opposite sign to V_1, V_2 so as to induce a sign-changing order parameter between the two sheets.

We now consider the scattering from nonmagnetic impurities. As discussed by Refs. 34–36, it is convenient to parameterize the scattering potential in terms of an amplitude U_{22}, describing scattering $\mathbf{k}\to\mathbf{k}'$ on the α sheet, similarly U_{11} on the β sheet, and $U_{12,21}$ between the two, such that the Born self-energy becomes

$$\underline{\Sigma}(\mathbf{k}\in 1,\omega) = n_I\left[\sum_{\mathbf{k}'\in 1}|U_{11}|^2\underline{G}(\mathbf{k}',\omega) + \sum_{\mathbf{k}'\in 2}|U_{12}|^2\underline{G}(\mathbf{k}',\omega)\right], \quad (15)$$

and similarly for $\mathbf{k}\in 2$. To compare the one-band and two-band cases, we now choose pairing parameters such that the order parameter on the β sheet is nearly identical to that we had in the one-band case above with $r_{\text{eff}} \equiv (\Delta_{\max}-\Delta_{\min})/(\Delta_{\max}+\Delta_{\min})=1.3$. This is illustrated as the pure spectral gap Ω_G in Fig. 7, where the corresponding isotropic gap on the α sheet is also shown. As disorder is added, the nodes are removed from the β sheet, as before, and a full gap created. At the same time the α gap is only very slightly

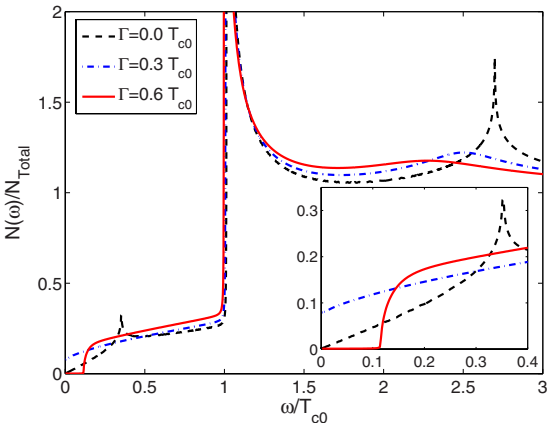

FIG. 8. (Color online) Density of states $N(\omega)/N_{\text{Total}}$ vs ω/T_{c0} for two-band system with $r_{\text{eff}}=1.3$. Same parameters and line types as in Fig. 7. Inset: expanded low-energy region.

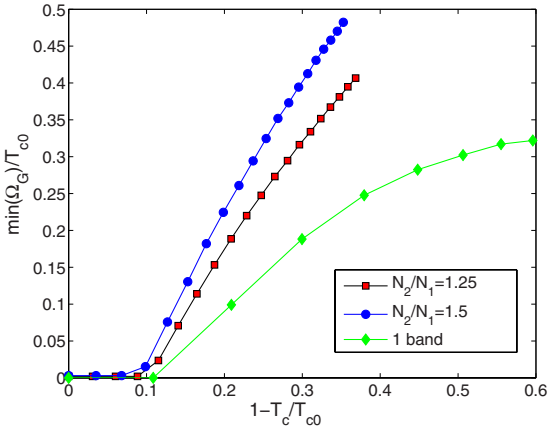

FIG. 9. (Color online) Normalized spectral gap min $\Omega_G(\phi)/T_{c0}$ vs T_c suppression $1-T_c/T_{c0}$ for various impurity concentrations comparing one-band and two-band models. Parameters are chosen such that $r_{\text{eff}}=1.3$ on the one (β) sheet for the pure superconducting state in all cases. Diamonds: one-band model with T_c/T_{c0} and Ω_G/T_{c0} taken from Figs. 2 and 3, respectively. Squares: two-band model with $V_{11}=1.0, V_{12}=-0.6, V_{22}=1.5$, with densities of states ratio $N_2(0)/N_1(0)=1.25$ and one sheet anisotropy parameter $r=1.76$. Circles: two-band model with same $V_{11}=1.0, V_{12}=-0.6, V_{22}=1.5$, but with densities of states ratio $N_2(0)/N_1(0)=1.5$ and $r=1.88$.

suppressed in this process. These features are evident also in the total DOS shown in Fig. 8 for the same scattering parameters.

Our aim in this section is to see if within a two-band picture one can understand qualitatively under what circumstances a substantial spectral gap can be opened on the Fermi surface without suppressing T_c substantially as in the simple one-band example. The naive hypothesis formulated above, that the presence of a more isotropic gap on a second Fermi-surface sheet is sufficient to "protect" T_c against intraband scattering, is not universally correct. This is because the order parameters on the two sheets are strongly coupled by the interband pair interaction. To illustrate which aspects of the problem are important for the relative proportion of gap creation relative to T_c suppression, we compare in Fig. 9 the gap created by a certain amount of disorder versus the corresponding suppression of T_c, for the one-band case and two two-band cases where the effective one sheet anisotropy r_{eff} is held fixed, but the ratio of the densities of states on the two sheets are varied. It is seen that the critical temperature is rendered more robust when the density of states $N_2(0)$, which controls the pairing weight on sheet 2(α), is increased. Any effect which enhances the nodeless sheet 2 pairing weight makes T_c less susceptible to intraband scattering. Thus we conclude that the amount of T_c suppression associated with gap creation depends on the details of the situation, and can become quite small.

The true Fermi-surface structure is of course more complicated than the two-sheet model considered here, so it is interesting to ask whether results from the more complete model show the desired effect. We show in Fig. 10 calculations for the spectral gap in the extended s-wave (A_{1g}) state obtained from the microscopic calculations of Ref. 29 for various values of intraband disorder scattering. The node-lifting phenomenon on the β sheets is clearly observed. In Fig. 11, we show that relatively little T_c suppression accompanies this realistic case; significant gaps of order $0.1-0.2T_c$ are obtained for $1-T_c/T_{c0}$ of only $\sim 10\%$.

V. CONCLUSIONS

There is now evidence that the superfluid density has a T dependence consistent with a fully developed gap in some samples, while power laws in T, including linear T, have been reported in others. It is possible that parameters related to the electronic structure of the pure state tune the various materials such that different superconducting ground states are realized. This is "natural" due to the proximity of these systems to a situation where nearly circular Fermi-surface sheets nest perfectly, in which case spin-fluctuation theory predicts a degeneracy between the extended-s (A_{1g}) and d-wave (B_{1g}) states.

Here we have explored an alternative possibility which assumes that there are nodes in an extended-s-wave (A_{1g}) state for the ideal ferropnictide material, but that these nodes are lifted by small momentum disorder scattering. In this regard, it is interesting that the stoichiometric ferropnictide LaFePO (with a mean-free path of more than 1×10^2 nm and capable of supporting dHvA oscillations) displays a linear T dependence of the superfluid density at low temperatures. While many mechanisms can give rise to a power-law T dependence in the superfluid density, we are aware of only one explanation for a linear-T law, namely, the existence of nodes in the pure state. On this basis we speculate that the exponential behaviors observed in other materials are due to disorder. On the other hand, evidence for the opposite trend has been reported in the $Ba_{1-x}K_xFe_2As_2$ system, where the cleanest crystals appear to exhibit exponential T dependence, whereas more disordered samples exhibit a low-temperature dependence which mimics a power law.

We have therefore explored a scenario in which weak nodes in a sign-changing $s_{+/-}$ state on the β sheets of the ferropnictides are "lifted" by nonmagnetic disorder. Qualitative aspects of this phenomenon are obtainable already within a simple one-band model where weak pointlike scatterers are accounted for. With increasing disorder, the nodes

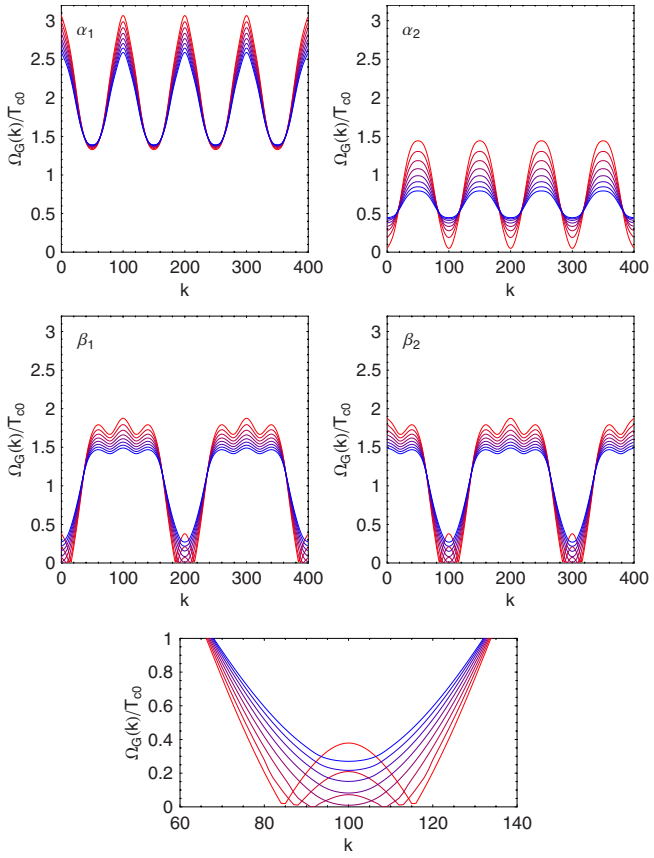

FIG. 10. (Color online) Spectral gap vs Fermi-surface arc length in arbitrary units on each of four Fermi-surface sheets (α_1, α_2, β_1, and β_2) for realistic spin-fluctuation model of Fig. 17 of Ref. 29. Curves correspond to an arbitrary range of impurity concentrations, from red (clean) to blue (dirty). Bottom panel: detail of nodal region of β sheets.

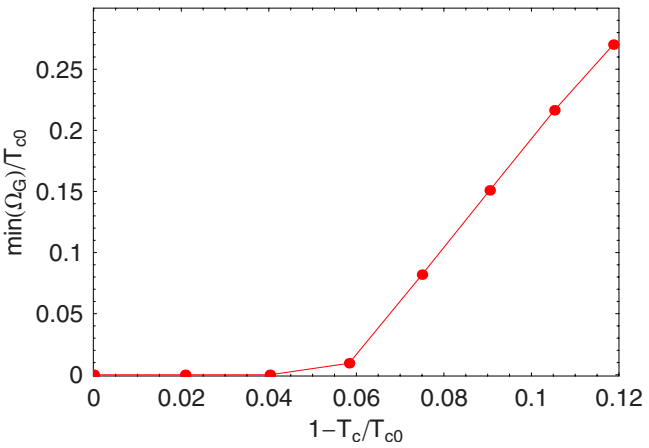

FIG. 11. (Color online) min Ω_G/T_{c0} vs $1-T_c/T_{c0}$ for same disorder parameters as Fig. 10.

disappear and are replaced by a fully developed gap and an activated temperature dependence of ρ_s. Thus one could imagine that the entire class of ferropnictide materials has intrinsic nodes in the ground-state order parameter of the analog pure system, which then disappear in most of the doped, much dirtier materials. We have shown that in the simplest model the lifting of the nodes corresponds to a significantly larger pair-breaking rate and concomitant T_c suppression than observed experimentally, but that this undesirable aspect of the theory is substantially eliminated by the consideration of additional bands with more isotropic pair state, as found in the microscopic theory.[29]

The justification for our neglect of interband scattering in most of this work is based on the empirical robustness of T_c to differences in sample quality, suggesting that interband scattering in the sign-changing s state is negligible. In addition, Yukawa-type models of realistic impurity potentials with finite range have small large-q amplitudes. Nevertheless, for a quantitative description of these materials both types of scattering should be considered, and a more microscopic understanding of the types of potentials introduced, e.g., by a K replacing Ba, Sr out of the FeAs plane and by a Co substituting directly for an Fe would be very useful.

The simple theory presented in Sec. II is actually applicable to a state with arbitrary anisotropy parameter r, allowing us to describe the pure d-wave state for $r \gg 1$, as well as a state with deep minima of the order parameter ("quasinodes"), but no true nodes for $r \lesssim 1$ as found, e.g., in Ref. 26. Thus we emphasize that it is possible that small differences in the electronic structure of different materials may give rise to slightly different gap structures, and even different symmetry classes[29] in different materials. The implication of current ARPES experiments, that the order-parameter anisotropy around the various Fermi-surface sheets is absent or very weak is, however, difficult to reconcile with experimental data, which indicate low-energy excitations, and a disorder-based explanation of the kind given here, where nodes or quasinodes are lifted by momentum averaging, seems to us the most likely way to understand the existing data. This picture will have implications for other properties, including transport properties, as discussed in Ref. 54 for the one-band situation, but there may be interesting modifications peculiar to the multiband case.

A remaining interesting question, which we have not yet studied in detail, is the effect of magnetic disorder, and in particular whether magnetic impurities can lift the nodes of an A_{1g} state in a manner qualitatively similar to that described here. In general, one expects magnetic disorder to act much more strongly than nonmagnetic disorder to reduce the average gap value, but the momentum dependence of the gap will be smeared as well. Preliminary calculations suggest that magnetic disorder cannot lift nodes for the types of states we have considered. Further work along these lines is in progress.

We note in closing that an alternative approach to the Fe pnictides takes the point of view that the intrinsic material is fully gapped with a sign-changing s-wave state, and that the inter-Fermi-surface scattering leads to the appearance of low-temperature power-law behavior. Clearly systematic electron irradiation or some other source of disorder which does not change the doping of the system would be a very important experimental way to distinguish this proposal from our own.

ACKNOWLEDGMENTS

The authors are grateful for useful communications with D.A. Bonn, J. Bobowski, and A. Carrington. Research was partially supported by DOE under Grant No. DE-FG02-05ER46236 (P.J.H.), and the Deutscheforschungsgemeinschaft (S.G.). T.A.M., D.J.S., and P.J.H. acknowledge the Center for Nanophase Materials Science, which is sponsored at Oak Ridge National Laboratory by the Division of Scientific User Facilities, U.S. Department of Energy.

[1] C. C. Tsuei and J. R. Kirtley, Rev. Mod. Phys. **72**, 969 (2000).
[2] Y. Kamihara, T. Watanabe, M. Hirano, and H. Hosono, J. Am. Chem. Soc. **130**, 3296 (2008).
[3] K. Hashimoto, T. Shibauchi, T. Kato, K. Ikada, R. Okazaki, H. Shishido, M. Ishikado, H. Kito, A. Iyo, H. Eisaki, S. Shamoto, and Y. Matsuda, Phys. Rev. Lett. **102**, 017002 (2009).
[4] L. Malone, J. D. Fletcher, A. Serafin, A. Carrington, N. D. Zhigadlo, Z. Bukowski, S. Katrych, and J. Karpinski, arXiv:0806.3908 (unpublished).
[5] C. Martin, R. T. Gordon, M. A. Tanatar, M. D. Vannette, M. E. Tillman, E. D. Mun, P. C. Canfield, V. G. Kogan, G. D. Samolyuk, J. Schmalian, and R. Prozorov, arXiv:0807.0876 (unpublished).
[6] K. Hashimoto *et al.*, arXiv:0810.3506 (unpublished).
[7] R. T. Gordon, N. Ni, C. Martin, M. A. Tanatar, M. D. Vannette, H. Kim, G. Samolyuk, J. Schmalian, S. Nandi, A. Kreyssig, A. I. Goldman, J. Q. Yan, S. L. Bud'ko, P. C. Canfield, and R. Prozorov, arXiv:0810.2295 (unpublished).
[8] R. T. Gordon, C. Martin, H. Kim, N. Ni, M. A. Tanatar, J. Schmalian, I. I. Mazin, S. L. Bud'ko, P. C. Canfield, and R. Prozorov, arXiv:0812.3683 (unpublished).
[9] J. D. Fletcher, A. Serafin, L. Malone, J. Analytis, J.-H. Chu, A. S. Erickson, I. R. Fisher, and A. Carrington, arXiv:0812.3858 (unpublished).
[10] L. Zhao *et al.*, Chin. Phys. Lett. **25**, 4402 (2008).
[11] H. Ding, P. Richard, K. Nakayama, T. Sugawara, T. Arakane, Y. Sekiba, A. Takayama, S. Souma, T. Sato, T. Takahashi, Z. Wang, X. Dai, Z. Fang, G. F. Chen, J. L. Luo, and N. L. Wang, Europhys. Lett. **83**, 47001 (2008).
[12] T. Kondo, A. F. Santander-Syro, O. Copie, C. Liu, M. E. Tillman, E. D. Mun, J. Schmalian, S. L. Bud'ko, M. A. Tanatar, P. C. Canfield, and A. Kaminski, Phys. Rev. Lett. **101**, 147003 (2008).
[13] D. V. Evtushinsky, D. S. Inosov, V. B. Zabolotnyy, A. Koitzsch, M. Knupfer, B. Buchner, G. L. Sun, V. Hinkov, A. V. Boris, C. T. Lin, B. Keimer, A. Varykhalov, A. A. Kordyuk, and S. V. Borisenko, Phys. Rev. B **79**, 054517 (2009).
[14] K. Nakayama, T. Sato, P. Richard, Y.-M. Xu, Y. Sekiba, S. Souma, G. F. Chen, J. L. Luo, N. L. Wang, H. Ding, and T. Takahashi, arXiv:0812.0663 (unpublished).
[15] L. Wray, D. Qian, D. Hsieh, Y. Xia, L. Li, J. G. Checkelsky, A. Pasupathy, K. K. Gomes, C. V. Parker, A. V. Fedorov, G. F. Chen, J. L. Luo, A. Yazdani, N. P. Ong, N. L. Wang, and M. Z. Hasan, Phys. Rev. B **78**, 184508 (2008).
[16] R. Klingeler, N. Leps, I. Hellmann, A. Popa, C. Hess, A. Kondrat, J. Hamann-Borrero, G. Behr, V. Kataev, and B. Buechner, arXiv:0808.0708 (unpublished).
[17] K. Matano, Z. A. Ren, X. L. Dong, L. L. Sun, Z. X. Zhao, and G.-q Zheng, EPL **83**, 57001 (2008).
[18] H.-J. Grafe, D. Paar, G. Lang, N. J. Curro, G. Behr, J. Werner, J. Hamann-Borrero, C. Hess, N. Leps, R. Klingeler, and B. Buchner, Phys. Rev. Lett. **101**, 047003 (2008).
[19] K. Ahilan, F. L. Ning, T. Imai, A. S. Sefat, R. Jin, M. A. McGuire, B. C. Sales, D. Mandrus, Phys. Rev. B **78**, 100501(R) (2008).
[20] Yusuki Nakai, Kenji Ishida, Yoichi Kamihara, Masahiro Hirano, and Hideo Hosono, J. Phys. Soc. Jpn. **77**, 073701 (2008).
[21] L. Shan, Y. Wang, X. Zhu, G. Mu, L. Fang, C. Ren, and H.-H. Wen, Europhys. Lett. **83**, 57004 (2008).
[22] T. Y. Chen, Z. Tesanovic, R. H. Liu, X. H. Chen, and C. L. Chien, Nature (London) **453**, 1224 (2008).
[23] D. Daghero, M. Tortello, R. S. Gonnelli, V. A. Stepanov, N. D. Zhigadlo, and J. Karpinski, arXiv:0812.1141 (unpublished).
[24] R. S. Gonnelli, D. Daghero, M. Tortello, G. A. Ummarino, V. A. Stepanov, J. S. Kim, and R. K. Kremer, arXiv:0807.3149 (unpublished).
[25] K. Kuroki, S. Onari, R. Arita, H. Usui, Y. Tanaka, H. Kontani, and H. Aoki, Phys. Rev. Lett. **101**, 087004 (2008).
[26] F. Wang, H. Zhai, Y. Ran, A. Vishwanath, and D.-H. Lee, Phys. Rev. Lett. **102**, 047005 (2009).
[27] I. I. Mazin, D. J. Singh, M. D. Johannes, and M. H. Du, Phys. Rev. Lett. **101**, 057003 (2008).
[28] A. V. Chubukov, D. V. Efremov, and I. Eremin, Phys. Rev. B **78**, 134512 (2008).
[29] S. Graser, T. A. Maier, P. J. Hirschfeld, and D. J. Scalapino, New J. Phys. **11**, 025016 (2009).
[30] C. Cao, P. J. Hirschfeld, H.-P. Cheng, Phys. Rev. B **77**, 220506(R) (2008).
[31] L. S. Borkowski and P. J. Hirschfeld, Phys. Rev. B **49**, 15404 (1994).
[32] R. Fehrenbacher and M. R. Norman, Phys. Rev. B **50**, 3495 (1994).
[33] G. Preosti and P. Muzikar, Phys. Rev. B **54**, 3489 (1996).
[34] A. A. Golubov and I. I. Mazin, Phys. Rev. B **55**, 15146 (1997).
[35] Y. Senga and H. Kontani, J. Phys. Soc. Jpn. **77**, 113710 (2008); Y. Senga and H. Kontani, arXiv:0812.2100 (unpublished).
[36] Y. Bang, H.-Y. Choi, and H. Won, arXiv:0808.3473 (unpublished).
[37] D. Parker, O. V. Dolgov, M. M. Korshunov, A. A. Golubov, and I. I. Mazin, Phys. Rev. B **78**, 134524 (2008).
[38] A. V. Chubukov, D. Efremov, and I. Eremin, Phys. Rev. B **78**, 134512 (2008).
[39] A. B. Vorontsov, M. G. Vavilov, and A. V. Chubukov, arXiv:0901.0719 (unpublished).
[40] D. Markowitz and L. P. Kadanoff, Phys. Rev. **131**, 563 (1963).
[41] A. A. Abrikosov and L. P. Gor'kov, Zh. Eksp. Teor. Fiz. **39**, 1781 (1960) [Sov. Phys. JETP **12**, 1243(1961)].
[42] L. P. Gorkov and P. A. Kalugin, JETP Lett. **41**, 208 (1985); **41**, 253 (1985).
[43] K. Ueda and M. Rice, in *Theory of Heavy Fermions and Valence*

Fluctuations, edited by T. Kasuya and T. Saso (Springer-Verlag, Berlin, 1985), p. 216.
[44] M. Sigrist and K. Ueda, Rev. Mod. Phys. **63**, 239 (1991).
[45] S. Skalski, O. Betbeder-Matibet, and P. R. Weiss, Phys. Rev. **136**, A1500 (1964).
[46] P. J. Hirschfeld, P. Wölfle, and D. Einzel, Phys. Rev. B **37**, 83 (1988).
[47] We have averaged the *xx* and *yy* components to simulate the ferropnictide with order parameters on β_1 and β_2 sheets rotated by $\pi/2$ in local coordinates with respect to one another.
[48] The approximate factor of 2 difference between the kink temperature and the antinodal order-parameter energy arises from the width of the thermal quasiparticle distribution.
[49] F. Gross, B. S. Chandrasekhar, D. Einzel, P. J. Hirschfeld, K. Andres, H. R. Ott, J. Beuers, Z. Fisk, and J. L. Smith, Z. Phys. B: Condens. Matter **64**, 175 (1986).
[50] I. Kosztin and A. J. Leggett, Phys. Rev. Lett. **79**, 135 (1997).
[51] Yoichi Kamihara, Hidenori Hiramatsu, Masahiro Hirano, Ryuto Kawamura, Hiroshi Yanagi, Toshio Kamiya, and Hideo Hosono, J. Am. Chem. Soc. **128**, 10012 (2006).
[52] A. I. Coldea, J. D. Fletcher, A. Carrington, J. G. Analytis, A. F. Bangura, J. H. Chu, A. S. Erickson, I. R. Fisher, N. E. Hussey, and R. D. McDonald, Phys. Rev. Lett. **101**, 216402 (2008).
[53] P. J. Hirschfeld and N. Goldenfeld, Phys. Rev. B **48**, 4219 (1993).
[54] L. S. Borkowski, P. J. Hirschfeld, and W. O. Putikka, Phys. Rev. B **52**, R3856 (1995).